ResearchGate

Laminar non-Newtonian open channel flow: Investigating velocity, wall shear stress and fluid depth.

Conference Paper · September 2010

3 authors:

J. H. Burger
Cape Peninsula University of Technology

Rainer Haldenwang
Cape Peninsula University of Technology

Neil Alderman

Laminar non-Newtonian open channel flow: Investigating velocity, wall shear stress and fluid depth

Johan Burger, Rainer Haldenwang
Flow Process Research Centre, Cape Peninsula University of Technology, Cape Town South Africa

Neil Alderman
BHR Group Ltd, Cranfield, Bedfordshire, UK

Data for laminar non-Newtonian flow in various non-circular open channels can be described by a general relationship, $f = K/\mathrm{Re}_H$ where f is the friction factor and Re_H is the appropriate Haldenwang et al (1) Reynolds number corresponding to the rheological model used to describe the non-Newtonian behaviour exhibited by the test fluid. The K values were found to range from 14.6 to 17.6 depending on the channel shape used and to be similar to those reported for Newtonian flow (2).

Despite the good agreement of $f = K/\mathrm{Re}_H$ line with the data found for each channel shape, this paper outlines the concerns regarding the comparison of actual and predicted velocities, the comparison of measured and predicted wall stresses and the flow depth sensitivity. In terms of velocity, wall shear stress and flow depth prediction, the Haldenwang et al (1) model was found to hold reasonably well for power law fluids. However, this was not the case for Bingham plastic and Herschel-Bulkley fluids. A possible reason for these discrepancies may be due to the contribution of the yield stress not being properly accounted for in the flow modelling.

NOTATION

A	-	cross sectional area for flow	m^2
B	-	channel width	m
f	-	Fanning friction factor	
g	-	acceleration due to gravity	m/s^2
h	-	fluid depth in channel	m
k	-	fluid consistency index	$Pa.s^n$
K	-	numerical constant dependent on channel shape	
n	-	flow behaviour index	
P	-	wetted perimeter of channel	m
Re	-	Newtonian Reynolds number	
Re_H	-	Haldenwang Reynolds number, Eqn (6)	
R_h	-	hydraulic radius	m
V	-	average velocity	m/s
α	-	subtended angle of semi-circular cross-section, Figure 1	degrees
η	-	Newtonian viscosity	Pa s
θ	-	channel angle from the horizontal	degrees
ρ	-	density	kg/m^3

τ_w	-	wall shear stress	Pa
τ_y	-	yield stress	Pa

1 INTRODUCTION

Open channels, flumes or launders are used in the mining industry to transport mineral ore slurries or tailings to waste disposal sites. With open channel flow being a gravity driven process, the design of these channels is highly dependent on the available slope for flow. Mountainous terrain such as the Andes in Chile and Peru often provide ample gradient for channel flow over large distances. In these locations, the transportation of tailings is usually performed in turbulent flow where the flow depth is reasonably constant.

However, with water becoming a scarce and expensive resource, there has been a demand for significant reduction of water used in tailings preparation. With the requirement of tailings being transported at higher concentrations, this causes the slurry to become more non-Newtonian in nature to the extent that the flow in the channel is no longer turbulent. In laminar flow, the flow depth can change dramatically depending on the slurry rheological properties. If the slurry exhibits viscoplastic behaviour, the impact on the flow depth is further complicated by the presence of a yield stress that must be overcome for slurry flow.

2 LAMINAR NON-NEWTONIAN OPEN CHANNEL FLOW

Laminar flow of non-Newtonian flow in open channels of various cross-sectional shapes is of interest to several industries including the mining and minerals, paper and pulp, wastewater and food industries. The database for non-Newtonian flow in rectangular open channels developed by the Flow Process Research Centre (FPRC) at the Cape Peninsula University of Technology (3,4) was recently extended to include non-Newtonian flow in open channels of semi-circular, triangular and trapezoidal cross-sections (5). Prior to the publication of this database, only limited experimental datasets were available. Coussot (6) provided data for the flow of kaolin suspensions in rectangular and trapezoidal channels whereas Naik (7) obtained data for flow of kaolin suspensions in a rectangular flume. Wang and Plate (8) and Wang (9) carried out experimental studies on the flow of clay suspensions in rectangular channels. Fitton (10, 11) obtained data for flow of three different non-Newtonian fluids in semi-circular channels. Fitton (10,11), Spelay et al. (12) and Spelay (13) used the FPRC database for verification purposes in their work.

As for pipe flow, open channel flow data can be presented in the form of a Moody chart where the Fanning friction factor, f is plotted against Reynolds number, Re allowing laminar, transitional or turbulent flow regimes to be identified (14,15), Here, f is given by

$$f = \frac{2gR_h \sin\theta}{V^2} \tag{1}$$

with Re being the Newtonian Reynolds number given by

$$\mathrm{Re} = \frac{\rho V 4 R_h}{\eta} \quad (2)$$

in which the hydraulic radius, R_h is defined as

$$R_h = \frac{A}{P} \quad (3)$$

where A is the cross-sectional area for flow and P is the wetted perimeter of the channel.

Along with the experimental data, Straub et al (14) presented a theory for laminar flow of Newtonian fluids in open channels with various cross-sections. They showed that the data in the laminar flow regime is defined by a general relationship

$$f = \frac{K}{\mathrm{Re}} \quad (4)$$

where K is a numerical constant dependent on the channel shape. Analytical and numerical solutions for K were provided for a range of different cross-sectional shapes.

Very little has been reported in the literature for predicting non-Newtonian laminar flow in open channels of arbitrary cross-section. The earliest method was that proposed by Kozicki and Tiu (16,17) who generalised the Rabinowitsch-Mooney equation applicable to pipe and slit flow for laminar flow of power law and Bingham plastic fluids in non-circular channels. Following the approach of by Kozicki and Tiu (16,17), Coussot (6) derived expressions for laminar flow of a Herschel-Bulkley fluid in rectangular and trapezoidal channels. Unfortunately, these expressions were found to be erroneous since they did not contain the power law exponent anywhere within the expressions. By introducing a new Reynolds number based on the Herschel-Bulkley model adapted from the pipe Reynolds number presented by Slatter (18), Haldenwang et al (1) proposed an equation for the friction factor-Reynolds number relationship for laminar flow of non-Newtonian fluids in non-circular open channels. This was given by

$$f = \frac{16}{\mathrm{Re}_H} \quad (5)$$

where Re_H is given by

$$\mathrm{Re}_H = \frac{8 \rho V^2}{\tau_y + k\left(\dfrac{2V}{R_h}\right)^n} \quad (6)$$

An advantage of using this Reynolds number is that it can also be used for fluids exhibiting Newtonian, power law and Bingham plastic behaviour. Through the use of equation (6), they found that the laminar flow data of three different non-Newtonian fluids in rectangular open channels did collapse onto the $f = 16/\mathrm{Re}_H$ line. However, Burger et al (2) found the pipe flow paradigm of $f = 16/\mathrm{Re}_H$ used by Haldenwang et al

(1,19) for non-Newtonian flow in open channels of different cross-sectional shapes was incorrect. Instead, they found the use of Haldenwang et al (1) definition for Re given by equation (6) in the f vs Re relationship as defined by equation (4) was more appropriate in describing non-Newtonian flow in non-circular open channels. This relationship is given by

$$f = \frac{K}{\mathrm{Re}_H} \tag{7}$$

For the three non-Newtonian fluids in four different channels studied, they found the K values to be 14.6 for triangular channels with a vertex angle of 90^o, 16.2 for semi-circular channels, 16.4 for rectangular channels and 17.6 for trapezoidal channels with 60^o sides. These values agree well with those found by Straub et al (14) and Chow (15) for open channel flow of Newtonian fluids except for the trapezoidal channel, for which K = 15 resulted from numerical analysis.

Alderman & Haldenwang (20) carried out a limited comparative study between the various models for the prediction of laminar flow of power law, Bingham plastic and Herschel-Bulkley fluids in rectangular open channels using the data from the FPRC database. They concluded that the Haldenwang et al (1) model was the better model of the available models. Despite the good agreement of this model with the $16/\mathrm{Re}_H$ line for all three non-Newtonian fluids, they found that this model only gave a good agreement between the predicted and actual velocities for power law fluids. The large scatter observed between the predicted and actual velocities for Bingham plastic and Herschel-Bulkley fluids was attributed to the yield stress as a parameter in the velocity calculation. Since Burger et al (2) found the use of the Haldenwang et al (1) model to be inappropriate for non-Newtonian flow in open channels of different cross-sectional shapes, this paper reports on the comparison of actual and predicted velocities and the comparison of measured and predicted wall shear stresses based on the f vs Re relationship as defined by Eqn (7). In addition, the influence of the measured flow depth on these comparisons will be commented upon.

3 EXPERIMENTAL

The tests were carried out in a 10 m long tilting flume designed and built by the Flow Process Research Centre at the Cape Peninsula University of Technology. Further details of this flume can be found in Haldenwang (3). This flume can be hydraulically tilted at various angles up to 5 degrees from the horizontal. The width of this rectangular flume can be changed from 300 to 150 mm by placing a partition mid-section lengthways down the flume. By inserting an appropriate cross sectional insert, the rectangular flume can be changed into a flume with a triangular, semi-circular or trapezoidal cross-section. The various flume shapes with their dimensions used in this study are shown in Figure 1.

Flow curve measurements of the test material were also made in-situ during the flume test using an in-line tube viscometer fitted with three tubes of different diameters, 13, 28 and 80 mm. Each of the three tubes was fitted with an electromagnetic flow meter and two differential pressure transducers across a fixed length. Calibration with water gave an error of less than 10% for both the flow rate and the pressure drop (3).

Section	Size	Cross-sectional area A	Wetted perimeter P	Surface width W
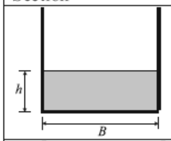	B = 300 mm B = 150 mm	Bh	$B + 2h$	B
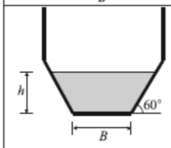	B = 150 mm B = 75 mm	$h(B+xh)$ where $x = 1/\tan 60^0$	$B + 2h\sqrt{1+x^2}$ where $x = 1/\tan 60^0$	$B + 2xh$ where $x = 1/\tan 60^0$
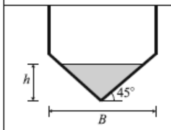	B = 300 mm	h^2	$2h\sqrt{2}$	2h
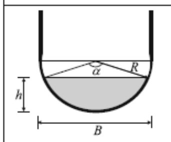	B = 300 mm B = 150 mm	$\frac{D^2}{8}(\alpha - \sin\alpha)$ where $\alpha = 2\cos^{-1}\left(1 - \frac{2h}{D}\right)$	$D\left(\frac{1}{2}\alpha\right)$ where $\alpha = 2\cos^{-1}\left(1 - \frac{2h}{D}\right)$	$D\left(\sin\frac{1}{2}\alpha\right)\alpha$ where $\alpha = 2\cos^{-1}\left(1 - \frac{2h}{D}\right)$

Figure 1. Flume shapes used in this study

A summary of the three different non-Newtonian fluids of varying concentrations used in the testwork can be found in Burger et al (2,5). For these materials, the flow curve data from the three different tube diameters were found to collapse onto a single curve thus confirming the absence of wall-slip during the flow curve measurement. Various model fits were then made to the flow curve data. It was found that the data for 1.5 to 5.3% v/v carboxymethylcellulose (CMC) solutions, 3.5 to 6.2% v/v bentonite in water suspensions and 3.4 to 9.2% v/v kaolin in water suspensions were best represented by the power law, Bingham plastic and Herschel-Bulkley models respectively. The correlation coefficient was used here as the criterion for determining the best model fit. This analysis also showed errors in the wall shear stress and wall shear rate to be very small (typically 0.1% and 0.6% of the wall shear stress and the wall shear rate values respectively). These findings are consistent with those found by Slatter (18) who used the same range of materials in his pipeflow studies.

The flow, provided by a 100 mm progressive cavity, positive displacement pump and a Warman 4x3 centrifugal slurry pump, was monitored by an electromagnetic flow meter. The maximum flow rate achieved was 45 l/s. Flow depths were measured with digital depth gauges of ±5% accuracy fitted at the 5 and 6 m positions from the flume entrance. These two positions were found to be the optimum for depth measurement (3). Since the difference in fluid depth between these two points was found to be minimal, the flow in this region can therefore be taken as steady.

A data logger was used to record the various data outputs as a function of time. All data were then fed to a PC so that a Moody chart could be generated as output.

4 RESULTS

Using all the experimental data for laminar flow of three different non-Newtonian fluids of varying concentrations in each of the four channels of varying dimensions and slopes, a f vs Re_H plot was obtained for each channel shape (2). These plots are reproduced in Figures 2 to 5 for rectangular, semi-circular, triangular and trapezoidal open channels respectively.

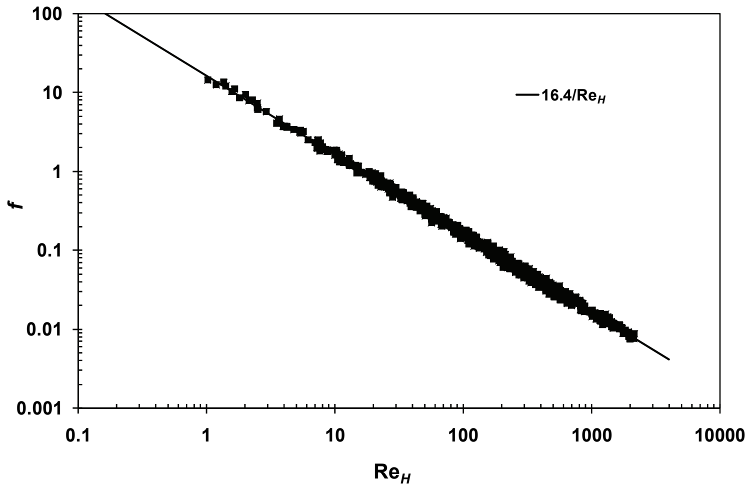

Figure 2. A f vs Re_H plot showing 647 data points for laminar flow of three different non-Newtonian fluids in a rectangular flume at slope angles of 1 to 5°.

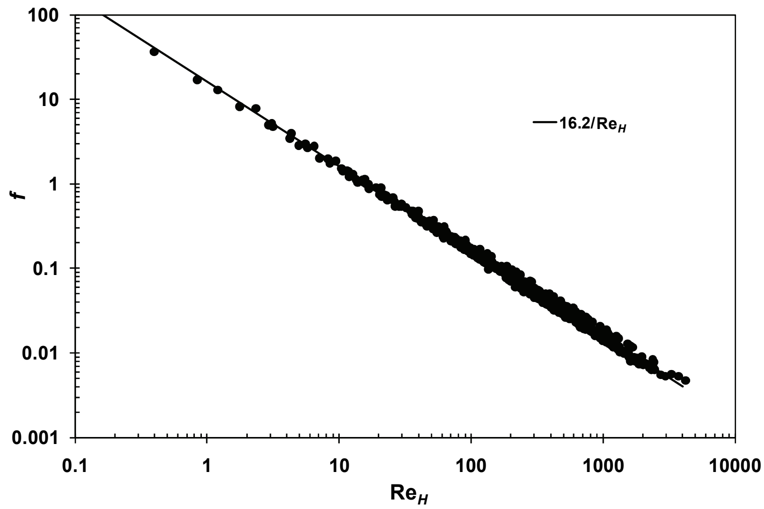

Figure 3. A f vs Re_H plot showing 485 data points for laminar flow of three different non-Newtonian fluids in a semi-circular flume at slope angles of 1 to 5°.

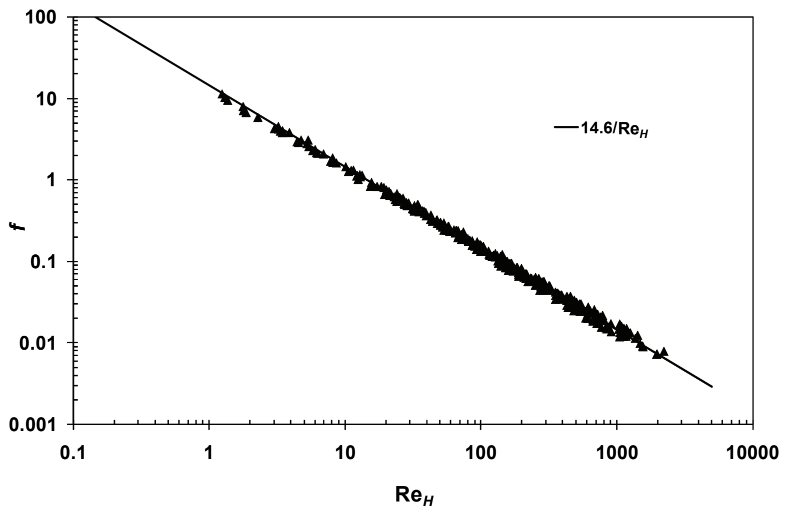

Figure 4. A *f* vs Re$_H$ plot showing 326 data points for laminar flow of three different non-Newtonian fluids in a triangular flume at slope angles of 1 to 5°.

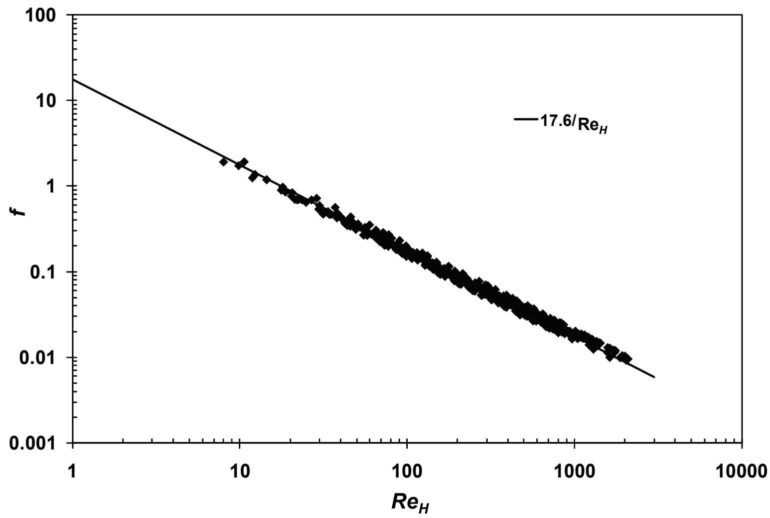

Figure 5. A *f* vs Re$_H$ plot showing 460 data points for laminar flow of three different non-Newtonian fluids in a trapezoidal flume at slope angles of 1 to 5°.

It can be seen from these plots that most of the experimental data do collapse onto a master curve. This was found by Burger et al (2) to be within 1.2 to 1.6 SD (standard deviation) of the average K value. They also concluded these K values agreed with those reported for open channel Newtonian flow (Straub et al., (14) and Chow, (15)) as opposed to the Haldenwang et al. (1,19) assumption of using a constant value of 16 for all channel shapes.

This paper expands the work of Burger et al (2) to report on the

(1) comparison of actual and predicted velocities where the actual velocity is simply the volumetric flow rate divided by the flow cross-sectional area and the predicted velocity is given by the appropriate equation for the model given by Eqn (7) using measured values of R_h and τ_w $(= R_h \rho g \sin \theta)$.

(2) comparison of measured and predicted wall shear stresses where the measured wall stress is given by $\tau_w = R_h \rho g \sin \theta$ and the predicted wall shear stress is given by the appropriate equation for the model given by Eqn (7) using measured values of R_h and V.

Good agreement between the velocity and wall shear stress comparisons will reaffirm the validity of the model given by Eqn (7) for predicting non-Newtonian flow in open channels of various cross-sectional shapes. Putting aside the different models given by Eqns (5) and (6) used for flow of three different non-Newtonian fluids in rectangular open channels, Alderman and Haldenwang (20) did demonstrate that the velocity comparison did not always hold well despite the good agreement of the model with the $16/Re_H$. This was especially true for Bingham and Herschel-Bulkley fluids.

In addition, the sensitivity of the flow depth measurement on open channel flow is discussed.

4.1 Comparison of actual and predicted velocities

Using the datasets for flow of 4 to 5% v/v CMC solutions in four different shaped channels, the actual and predicted velocities for a typical power law fluid are compared in Figure 6. This comparison shows that there is a ±20% variation between the actual and predicted velocities as shown by the dotted lines. Similar levels of variation were also observed for the other CMC solutions studied.

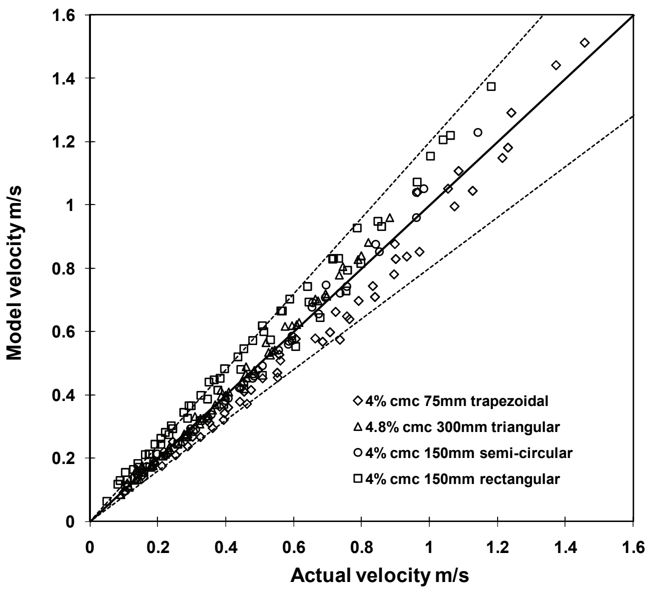

Figure 6. Velocity comparison for a typical power law fluid flowing in four different shaped channels.

For fluids exhibiting yield stress behaviour, a similar plot to Figure 6 was obtained using a selected range of datasets for flow of kaolin and bentonite suspensions in four different shaped channels. This is given in Figure 7 where it can be seen that there is a vast deviation between the actual and predicted velocities. Here, the error is in the region of ±1000%. This poor agreement is in spite of the good agreement of the K/Re_H line found by Burger et al (2). A possible cause of the large variation observed in Figure 7 is the introduction of the yield stress as a parameter in the calculation of the predicted velocities. Also from Figure 7, the residual errors in the velocity prediction appear to contain structure as opposed to random error resulting from a normal distribution of experimental error. This observation reinforces the contention that the yield stress does have a major influence on the velocity prediction.

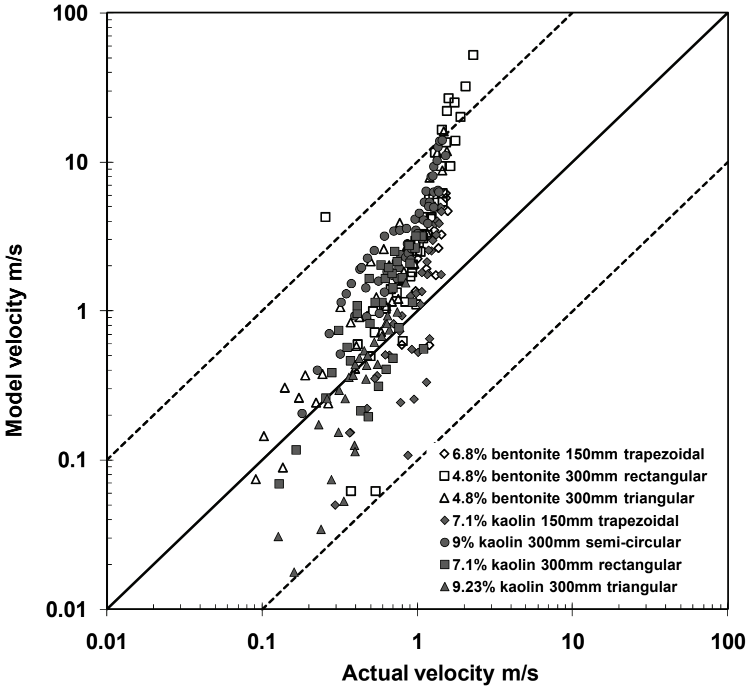

Figure 7. Velocity comparison for a range of yield stress fluids flowing in four different shaped channels.

4.2 Comparison of measured and predicted wall shear stresses

Using the same dataset used for Figure 6, the actual and predicted wall shear stresses for a typical power law fluid are compared in Figure 8. This comparison shows that there is a ±10% variation between the actual and predicted wall shear stresses. Similar levels of variation were also observed for the other CMC solutions studied.

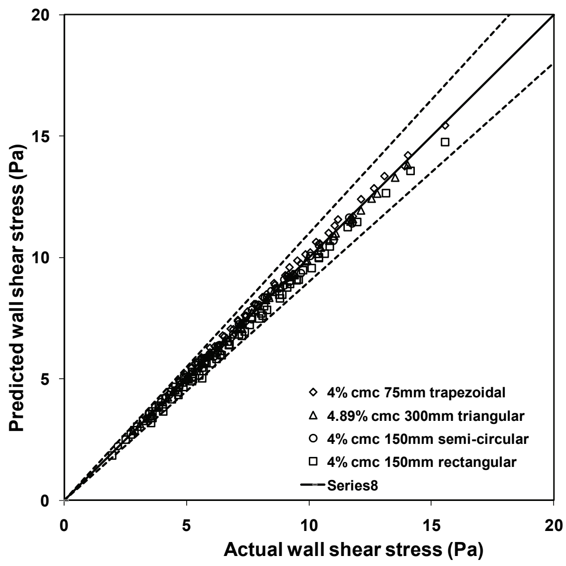

Figure 8. Wall shear stress comparison for a typical power law fluid flowing in four different shaped channels.

Using the same datasets in Figure 7, the actual and predicted wall shear stresses for a range of fluids exhibiting yield stress behaviour are compared in Figure 9. This comparison shows that there is a ±20% variation between the actual and predicted wall shear stresses, which can be regarded to be within experimental error.

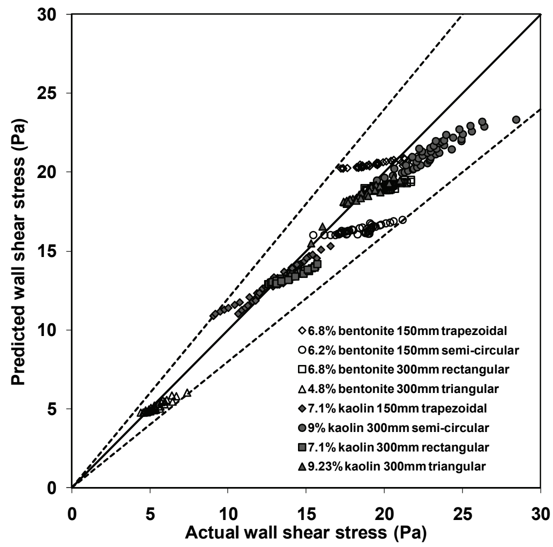

Figure 9. Wall shear stress comparison for a range of yield stress fluids flowing in four different shaped channels.

4.3 Flow depth sensitivity

During the experimental test work, it was observed that the flow depth is a very sensitive parameter especially when the flow depth was small. Plots of flow depth as a function of velocity and volume concentration were obtained for the three different non-Newtonian fluids flowing in four different shaped channels at slopes varying from 1 to 5°. Figure 10 depicts the variation of the initial flow depth with volume concentration at slope angles of 2° and 4°. It can be seen from this plot that for a given slope, this variation appears to be independent of the channel shape at low concentrations and dependent on the channel shape at higher concentrations. Taking the worst case, there is an overall increase in the flow depth of ~2700% and ~1200% when the channel slope is 2° and 4° respectively.

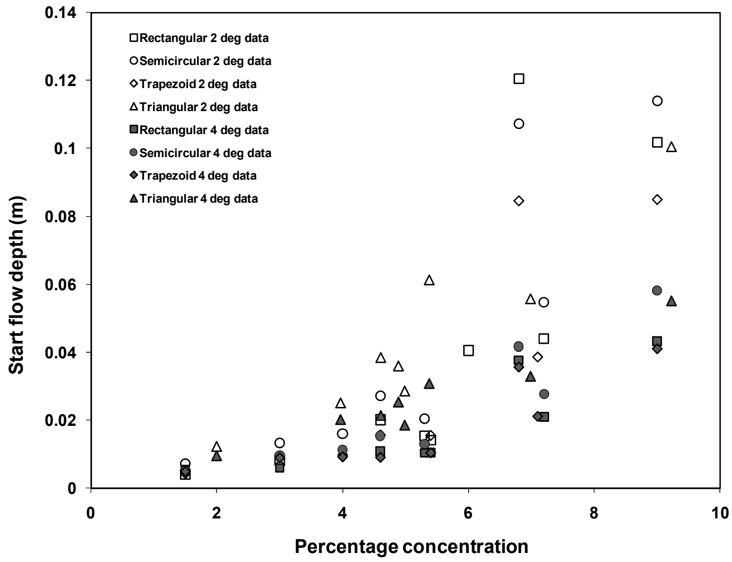

Figure 10. Initial flow depth versus volume concentration of three different non-Newtonian fluids flowing in four different shaped channels at slopes of 2° and 4°.

A similar plot to Figure 10 for the variation of flow depth with volume concentration at the onset of transition flow is given in Figure 11. Here, similar conclusions for Figure 10 can be applied for this plot except that for the worst case, there is an overall increase in the flow depth of ~2000% and ~880% when the channel slope is 2° and 4° respectively. Moreover, these two plots show the variation of flow depth with volume concentration is much more pronounced at 2° than for 4° due to the stronger influence of the fluid rheological properties on how the fluid flows down the channel.

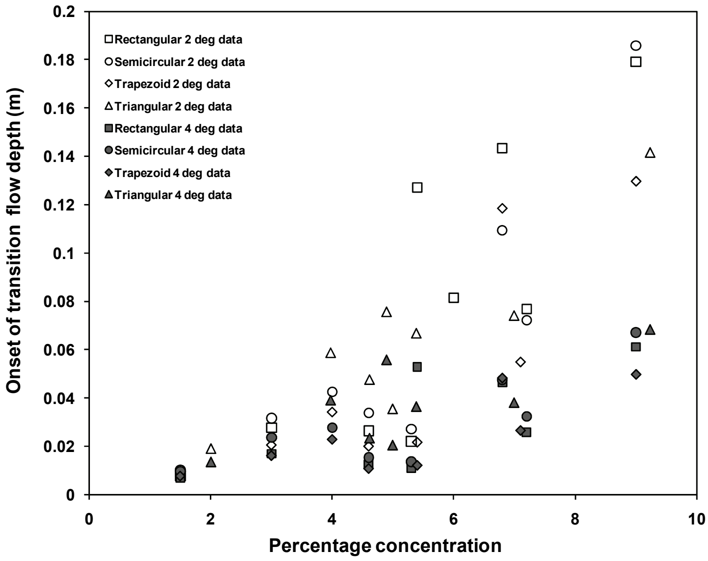

Figure 11. Onset of transition flow depth versus volume concentration of three different non-Newtonian fluids flowing in four different shaped channels at slopes of 2^{o} and 4^{o}.

Comparison between measured and predicted flow depths at the start of flow and at the onset of transition flow are shown in Figures 12 and 13 for power law and yield stress fluids respectively. It can be seen that that there is a ± 5% and ± 20% variation between the measured and predicted flow depths for power law and yield stress fluids respectively. The larger scatter observed in Figure 13 can be attributed to the contribution of the yield stress in the calculation of the wall shear stress when calculating the predicted flow depth but this contribution is not yet fully understood.

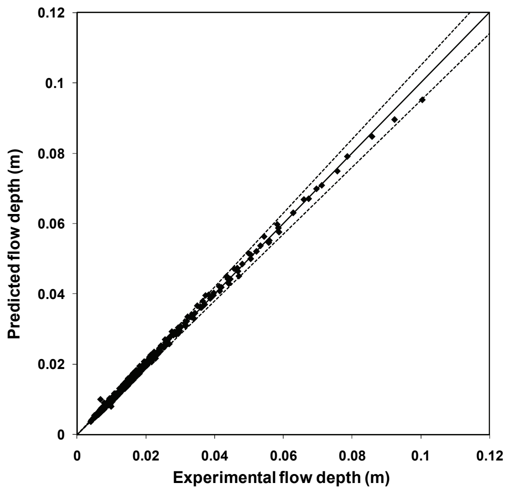

Figure 12. Predicted versus measured flow depth at start and end of laminar flow for CMC solutions flowing in four different shaped channels.

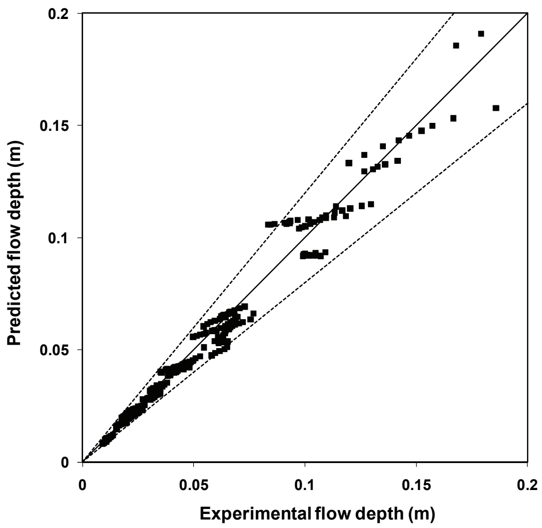

Figure 13. Predicted versus measured flow depth at start and end of laminar flow for kaolin and bentonite suspensions flowing in four different shaped channels.

5 CONCLUSIONS

Despite the good agreement of the $f = K/\mathrm{Re}_H$ line with the data found for rectangular, semi-circular, triangular and trapezoidal open channels shown in Figures 2 to 5 respectively, a closer inspection of the data revealed the following observations:

- For power law fluids, there is a ±20% variation between the actual and predicted velocities, a ±10% variation between the actual and predicted wall shear stresses and a ± 5% variation between the measured and predicted flow depths.
- For Bingham and Herschel Bulkley fluids, there is a ±1000% variation between the actual and predicted velocities and a ±20% variation between the actual and predicted wall shear stresses and the measured and predicted flow depths. The scatter is believed to be due to the contribution of the yield stress not being properly accounted for in the flow modelling.
- The variation of flow depth with volume concentration is more pronounced at lower slopes than that for higher slopes. This is especially true for fluids with a yield stress flowing down the channel when the slope is less than 2^o.

These observations would suggest a satisfactory design of open channels for laminar flow of power law fluids would be gained when using the Haldenwang et al model (1). However, this will not be the case for Bingham and Herschel-Bulkley fluids since further research is needed to underpin the role of yield stress in channel flow. To this end, veloci^{t}y profile measurements in a rectangular channel have been carried out using the ultrasound velocity profiling (UVP) method (21). Initial results indicate that it is possible to obtain velocity profiles of the three non-Newtonian fluids flowing in a channel over the whole cross-section. From these measurements, it is hoped that a better understanding of the flow of non-Newtonian fluids in open channels will be gained.

REFERENCES

(1) HALDENWANG, R., SLATTER, P.T. AND CHHABRA, R.P. (2002). Laminar and transitional flow in open channels for non-Newtonian fluids, In: Hydrotransport 15: 15th International Conference on the Hydraulic Transport of Solids in Pipes. Banff, Canada, Organised by BHR Group, Cranfield, Bedfordshire, UK, pp. 755-768.

(2) BURGER, J.H. HALDENWANG, R. AND ALDERMAN, N.J. (2010). Friction factor-Reynolds number relationship for laminar flow of non-Newtonian fluids in open channels of different cross-sectional shapes. *Chem. Eng. Sci.,* 65, 3549-3556.

(3) HALDENWANG, R. (2003). Flow of non-Newtonian fluids in open channels. Unpublished D. Tech. thesis. Cape Technikon, Cape Town, South Africa.

(4) HALDENWANG, R. AND SLATTER, P.T. (2006). Experimental procedure and database for non-Newtonian open channel flow. J. Hydraulic Res. 44(2), 283-287.

(5) BURGER, J., HALDENWANG, R. AND ALDERMAN, N. (2010). Experimental database for non-Newtonian flow in four channel shapes. *J. Hydraulic Res*. 48(3), 363–370.

(6) COUSSOT, P. (1994). Steady laminar flow of concentrated mud suspensions in open channels. *J. Hydraulic Res* 32(4), 535-558.

(7) NAIK, B. (1983). Mechanics of mudflow treated as the flow of a Bingham fluid. Unpublished *PhD thesis*. Washington State University.

(8) WANG, Z.-Y. AND PLATE, E.J. (1996). A preliminary study on the turbulence structure of flows of non-Newtonian fluid. *J. Hydraulic Res*. 34(3), 345-361.

(9) WANG, Z.-Y. (2002). Free surface instability of non-Newtonian laminar flows. *J. Hydraulic Res*. 40(4), 449-460.

(10) FITTON, T.G. (2007). Tailings beach slope prediction. Unpublished *PhD thesis*. Royal Melbourne Institute of Technology University, Melbourne, Australia.

(11) FITTON, T.G. (2008). Non-Newtonian open channel flow: A simple method of estimation of laminar/turbulent transition and flow resistance. *Paste* 2008, Kasane, Botswana, 245-251, A.B. Fourie, R.J. Jewell, A. Paterson., P.T Slatter, eds.

(12) SPELAY, R., SUMNER, R.J., SANDERS, R.S. AND GILLIES, R.G. (2006). Laminar open channel flow of kaolin clay slurries containing sand. 13th Intl. Conf. *Transport and sedimentation of solid particles*, Tbilisi, Georgia, 300-317.

(13) SPELAY, R. (2007). Solids transport in laminar, open channel flow of non-Newtonian slurries. Unpublished *PhD thesis*. University of Saskatchewan, Saskatoon, Canada.

(14) STRAUB, L.G., SILBERMAN, E. AND NELSON, H.C. (1958). Open channel flow at small Reynolds numbers, *Trans ASCE*, 123, 685 – 706.

(15) CHOW, V.T. (1959). *Open channel hydraulics*. McGraw-Hill, New York.

(16) KOZICKI, W. AND TIU, C. (1967). Non-Newtonian flow through open channels. *Can J Chem. Eng*., 45, 127-134.

(17) KOZICKI, W. AND TIU, C. (1986). Parametric modelling of flow geometries in non-Newtonian flows, In: Encyclopedia of Fluid Mechanics, Vol 7, ed N.P. Cheremisinoff, Gulf Publishing Co, Houston, pp.199 – 252.

(18) SLATTER, P.T. (1994). Transitional and turbulent flow of non-Newtonian slurries in pipes. Unpublished PhD thesis. University of Cape Town, Cape Town.

(19) HALDENWANG, R., SLATTER, P.T., VANYAZA, S. AND CHHABRA, R.P. (2004). The effect of shape on laminar flow in open channels for non-Newtonian fluids, In: Proc of Hydrotransport 16, 16th International Conference on Hydrotransport, Santiago, Chile, 26-28 April 2004. Organised by BHR Group, Cranfield, Bedfordshire, UK, pp. 311-325.

(20) ALDERMAN, N.J., HALDENWANG, R. (2007). A review of Newtonian and

non-Newtonian flow in rectangular open channels. *Hydrotransport* 17, The Southern African Institute of Mining and Metallurgy and the BHR Group, Cape Town, South Africa, 87-106.

(21) HALDENWANG, R., SLATTER, P.T., KOTZE, R and MARIETTE, O. (2006). An investigation in using UVP for assisting in rheological characterisation of mineral suspensions. ISUD 5. Fifth International Symposium on Ultrasound Doppler Methods for Fluid Mechanics and Fluid Engineering. Zurich, Switzerland. 77-80.